

Supporting Information

Revised November 23, 2010

Formation of a Dinuclear Imido Complex from the Reaction of a Ru^{VI} Nitride with a Ru^{II} Hydride

Xiao-Yi Yi,^{†,‡} Ho-Yuen Ng,[†] Ian D. Williams,[†] and Wa-Hung Leung^{*,†}

[†] *Department of Chemistry The Hong Kong University of Science and Technology, Clear Water Bay, Kowloon, Hong Kong, People's Republic of. China*

Fax: (+0852)2358 1594; E-mail: chleung@ust.hk

[‡] *School of Chemistry and Chemical Engineering, Central South University, Changsha, Hunan 410083, People's Republic of. China*

*Corresponding author.

1. Experimental Section

General Considerations. All manipulations were carried out under nitrogen by standard Schlenk techniques. Solvents were purified by standard procedures and distilled prior to use. NMR spectra were recorded on a Bruker ARX 400 spectrometer operating at 400 and 162 MHz for ^1H and ^{31}P , respectively. Chemical shifts (δ , ppm) were reported with reference to SiMe_4 (^1H) and H_3PO_4 (^{31}P), respectively. Infrared spectra were recorded on a Perkin-Elmer 16 PC FT-IR spectrophotometer. Mass spectra were recorded on an Applied Bio-system QSTAR spectrometer. Elemental analyses were performed by Medac Ltd., Surrey, UK. The complexes $[\text{Ru}(\text{L}_{\text{OEt}})(\text{N})\text{Cl}_2]$ (**1**)¹ and $[\text{Ru}(\text{L}_{\text{OEt}})(\text{H})(\text{CO})(\text{PPh}_3)]$ (**3**)² ($\text{L}_{\text{OEt}}^- = [\text{Co}(\eta^5\text{-C}_5\text{H}_5)\{\text{P}(\text{O})(\text{OEt})_2\}_3]^-$) were prepared as described elsewhere.

X-ray Crystallography. Crystal structure determinations: Diffraction data of complex **2** were recorded on a Bruker CCD diffractometer with monochromatized Mo-K α radiation ($\lambda = 0.71073\text{\AA}$) with crystals selected and mounted on glass fiber. The collected frames were processed with the software SAINT.^[3] Diffraction intensity data of complex **4** was collected on an Oxford Diffraction GeminiTMS Ultra with CCD Area Detector with monochromatized Cu-K α radiation ($\lambda = 1.54178\text{\AA}$) lattice determination. Data collection and reduction were carried out using CrysAlisPro 171.32.5. Absorption correction was performed using SADABS built-in the CrysAlisPro program suite.³ Structures were solved by direct methods and refined by full-matrix least-squares on F^2 using the SHELXTL software package.⁴ The atomic positions of non-hydrogen atoms were refined with anisotropic parameters. The H1B atom around N1 in **4** was located from the Fourier maps and was treated as riding atoms having isotropic displacement parameters related to N1 atom, and other hydrogen atoms were introduced at their geometric positions and refined as riding atoms.

The Crystallographic data, experimental details and selected bond distances and angles for complexes **2** and **4** are listed in Table S3, S4 and S5. For complex **2**, the pendant ethyl groups of the tripod ligands are disorder and have been refined with appropriate partial occupancies. For complex **4**, the Cp rings of the tripod ligand were found to be rotationally disordered and refined with occupancies of 0.65 and 0.35. The

five ethoxy groups in the L_{OEt}^- ligand and two phenyl rings of the PPh_3 ligand were also found to be disordered. Each of these carbon atoms were split into two sites with occupancies of 0.5 and 0.5, except for C17 and C18 atoms which were split into two sites with 0.6 and 0.4 occupancies.

CCDC-771482 (**2**) and 771481 (**4**) contain the supplementary crystallographic data for this paper. These data can be obtained free of charge via www.ccdc.cam.ac.uk/conts/retrieving.html (or from the Cambridge Crystallographic Data Centre, 12 Union Road, Cambridge CB2 1EZ, UK; fax: (+44) 1223-336-033; or deposit@ccdc.cam.ac.uk).

Synthesis of $[Ru(L_{OEt})Cl_2(NH_3)]$ (2**).** A mixture of complex **1** (72 mg, 0.1 mmol) and triethylsilane (70 mg, 0.6 mmol) in toluene (15 mL) was stirred at room temperature for 3 d. The solvent was removed by vacuum, and the yellow residue washed with hexane. Recrystallization from THF-hexane afforded yellow crystals which were suitable for X-ray diffraction study. Yield: (61 mg, 85%). IR (KBr, cm^{-1}): 3263 and 3333 (NH). μ_{eff} (Evans method, $CDCl_3$, 25 °C) = 1.79 μ_B . Anal. Calcd for $C_{17}H_{38}Cl_2CoNO_9P_3Ru$: C, 28.19; H, 5.29; N, 1.93; Found: C, 28.47; H, 5.50; N, 1.85.

Reaction of complex **1 with $n-Bu_3SnH$.** To a stirring solution of **1** (72 mg, 0.1 mmol) in toluene (5 mL) at -78 °C was added $n-Bu_3SnH$ (87 mg, 0.3 mmol) in toluene (10 mL) dropwise. The mixture was warmed to room temperature, at which it was stirred for 1 h. The solvent was removed by vacuum, and the residue was washed with hexane. Recrystallization from THF, ether/hexane was afforded a yellow solid which was identified as **2**. Yield: 40 mg (56 %).

Reaction of **1 with 4,4,5,5-tetramethyl-1,3,2-dioxaborolane.** To a solution of **1** (72 mg, 0.1 mmol) in toluene (8 mL) at 0 °C was added 4,4,5,5-tetramethyl-1,3,2-dioxaborolane (38 mg, 0.3 mmol) in toluene (5 mL) dropwise. The mixture was warmed to room temperature at which it was stirred for 3 h. The solvent was removed by vacuum, and the residue was washed with hexane. Recrystallization from toluene/hexane afforded a yellow solid which was identified as **2**. Yield: 30 mg (42 %)

Synthesis of $[(L_{OEt})Cl_2Ru(\mu-NH)Ru(CO)(PPh_3)(L_{OEt})]$ (4**):** To a solution of complex **1** (72 mg, 0.1 mmol) in toluene (4 mL) was added $[Ru(L_{OEt})(H)(CO)(PPh_3)]$ (93

mg, 0.1 mmol) in toluene (4 mL) and the mixture was stirred at room temperature for 4 h. After reducing the solution to ca. 1 mL, cool hexane (30 mL) was added to precipitate red solid of **4** (150 mg, 91%). Red crystals of **4** were from thf-hexane which were suitable for X-ray diffraction study. ¹H NMR (400 MHz, C₆D₆, 25 °C, TMS): δ 0.94 (6H, t, *J* = 5.6 Hz, CH₃), 1.12 (3H, t, *J* = 6.8 Hz, CH₃), 1.23-1.42 (24H, m, CH₃), 1.55 (3H, t, *J* = 6.8 Hz, CH₃), 3.02-3.11 (1H, m, CH₃), 3.25-3.35 (1H, m, CH₃), 3.61-3.71 (1H, m, CH₃), 3.89-4.03 (2H, m, CH₃), 4.05-4.90 (19H, m, CH₃), 4.93 (5H, s, Cp), 5.10 (5H, s, Cp), 7.06-7.13 (9H, m, PPh₃), 7.78 (6H, m, PPh₃) 40.6 (1H, s, NH) ppm. ³¹P NMR (162 MHz, C₆D₆, 25 °C, H₃PO₄): δ 45.0 (d, ³*J*_{PP} = 5.2 Hz, PPh₃), 107.5, 108.4, 108.9, 109.4, 109.8, 110.0, 110.7, 111.0, 112.2, 113.2, 113.6, 114.3, 116.8, 117.8, 118.8 (m, L_{OEt}) ppm. IR (KBr, cm⁻¹): 1949s (CO). Anal. Calcd for C₅₃H₈₆C₁₂Co₂NO₁₉P₇Ru₂: C, 38.61; H, 5.26; N, 0.85; Found: C, 38.75; H, 5.22; N, 0.77.

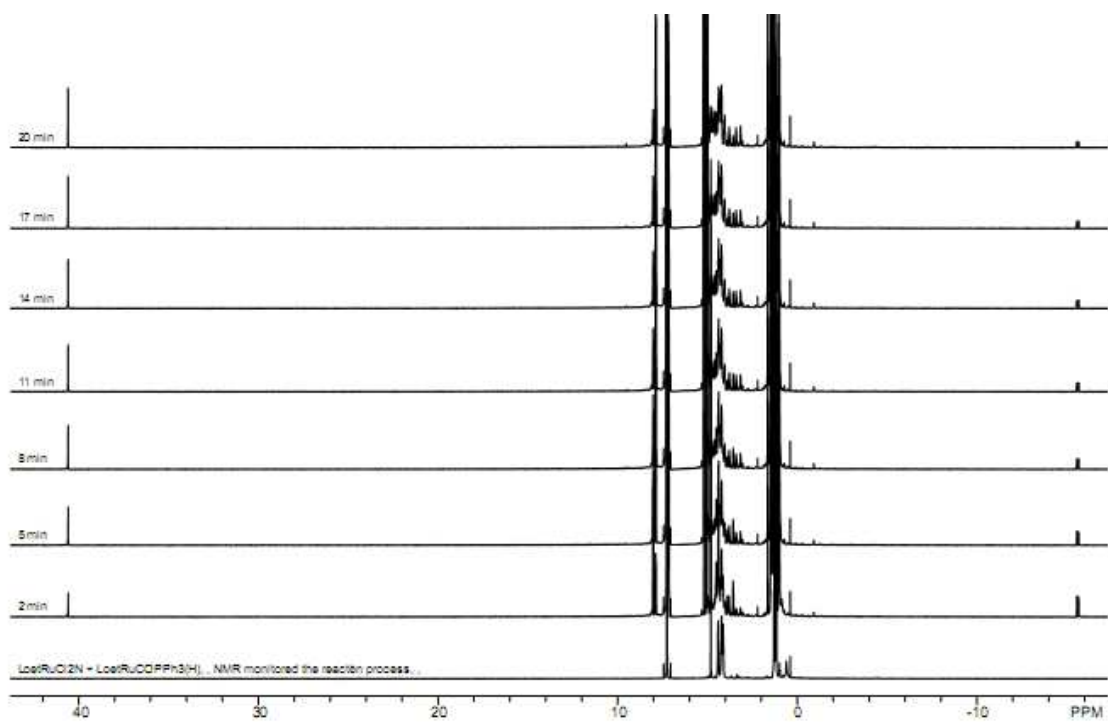
Kinetic studies of reaction of 1 and 3. The kinetics of the reaction was studied at 290.0 - 313.0 K under the pseudo-first-order conditions [**3**] >> [**1**]. Reactions were initiated by mixing **1** (2 μmol) with solution of **3** (20 μmol) in toluene (20 mL) under N₂. The reaction progress was monitored by observing absorbance change at 510 nm (Figure S1). Pseudo-first-order rate constants, *k*_{obs}, were obtained by nonlinear least-squares fit of *A_t* vs. time *t* according to the equation $A_t = A_f + (A_o - A_f)\exp(-k_{\text{obs}}t)$, where *A_o* and *A_f* are the initial and final absorbance, respectively (Figure S2). The plot of *k*_{obs} vs. [**3**] at 291.5 K is linear passing through the origin (Figure S3). Values of *k*_{obs} and *k*₂ for the reaction at 291.5 - 314.0 K are presented in Figure S4, Table S1 and Table S2, respectively.

References

- (1) Yi X.-Y.; Sau Y.-K.; Lam T. C. H.; Williams I. D.; Leung W.-H. *Inorg. Chem.* **2007**, *46*, 7193 – 7198.
- (2) Leung W.-H.; Chan E. Y. Y.; Wong W.-T. *Inorg. Chem.* **1999**, *38*, 136 – 143.
- (3) Bruker SMART and SAINT+, Version 6.02a, Siemens Analytical X-ray Instruments Inc., Madison, Wisconsin, USA, **1998**.
- (4) Sheldrick G. M. *SHELXTL-Plus V5.1 Software Reference Manual*; Bruker AXS Inc., Madison, Wisconsin, USA, **1997**.

Figure S1. ^1H NMR spectral change [in the (a) δ -18-44 ppm and (b) δ 3-9 ppm region] for the reaction of $[\text{Ru}(\text{L}_{\text{OEt}})(\text{N})\text{Cl}_2]$ (**1**) with 1.1 equiv of $[\text{Ru}(\text{L}_{\text{OEt}})(\text{H})(\text{CO})(\text{PPh}_3)]$ (**3**) in benzene- d_6 at room temperature (time interval = 3 min).

(a)



(b)

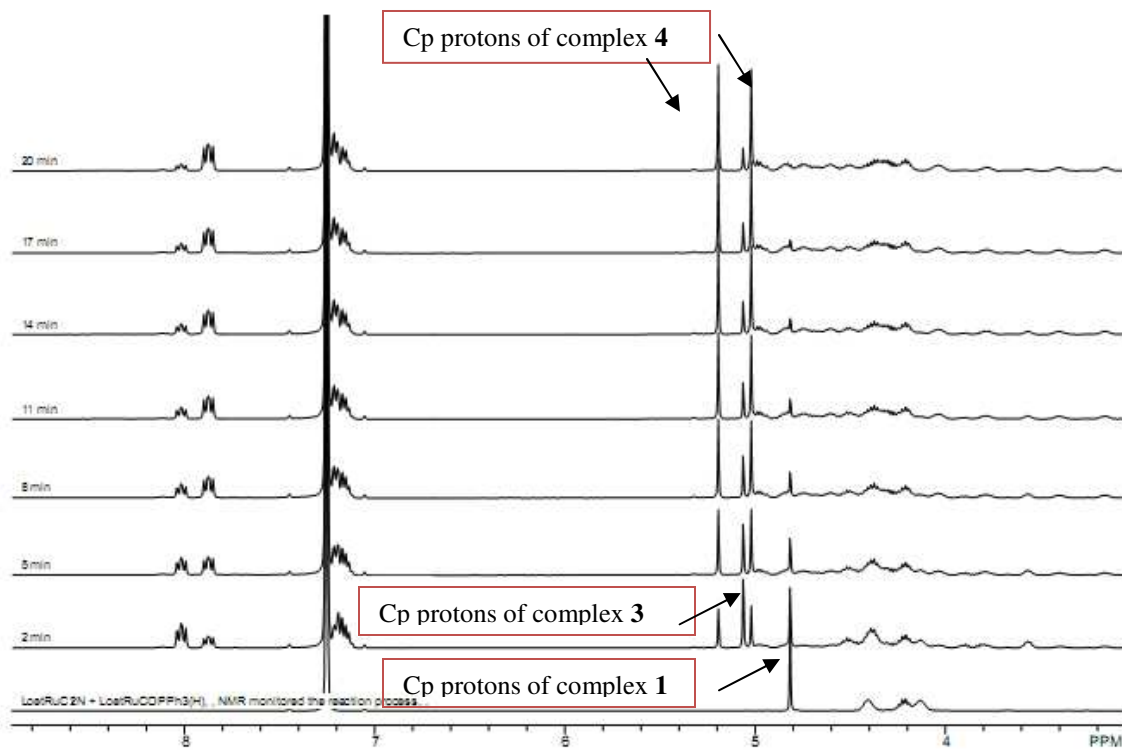
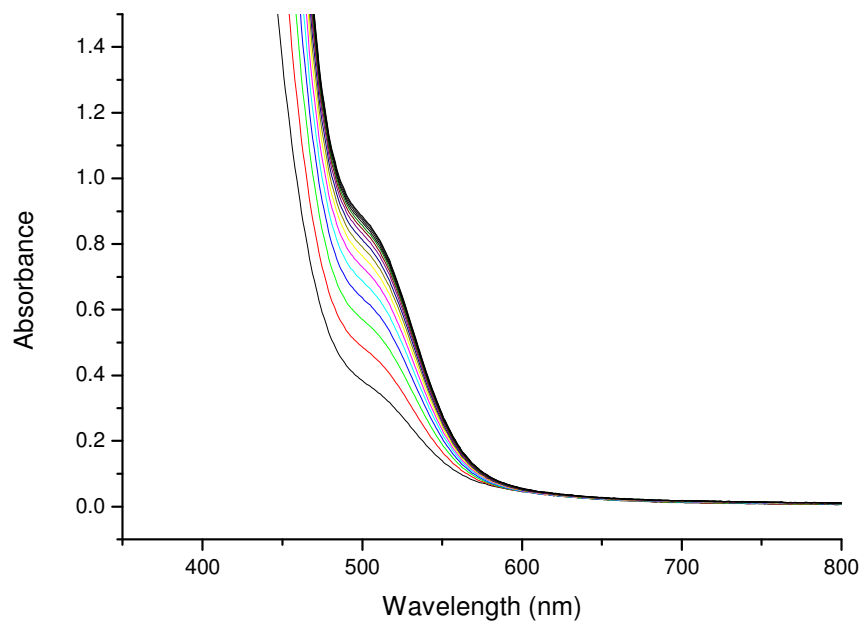


Figure S2. (a) UV-vis spectral change for the reaction of **1** with 15-fold excess **3** in toluene at 25 °C. (b) An expansion near the 510-nm region.

(a)



(b)

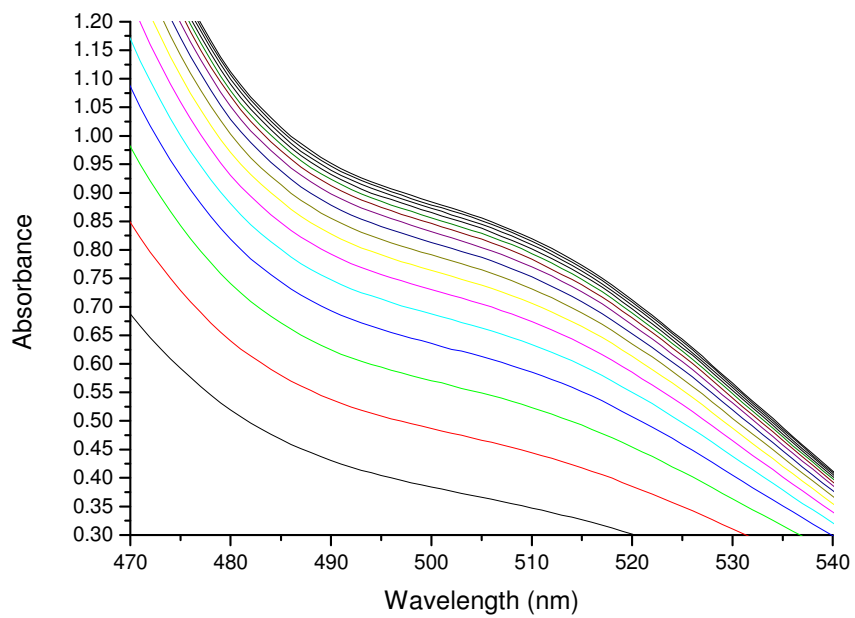


Figure S3. (a) Plot of $(A_t - A_o)/(A_f - A_o)$ vs. time. (b) Plot of $\ln[(A_f - A_t)/(A_f - A_o)]$ vs. time, (slope = k_{obs}) for the reaction of complexes **1** with **3**, under the pseudo-first-order conditions $[3] \gg [1]$ at 298 K in toluene solution.

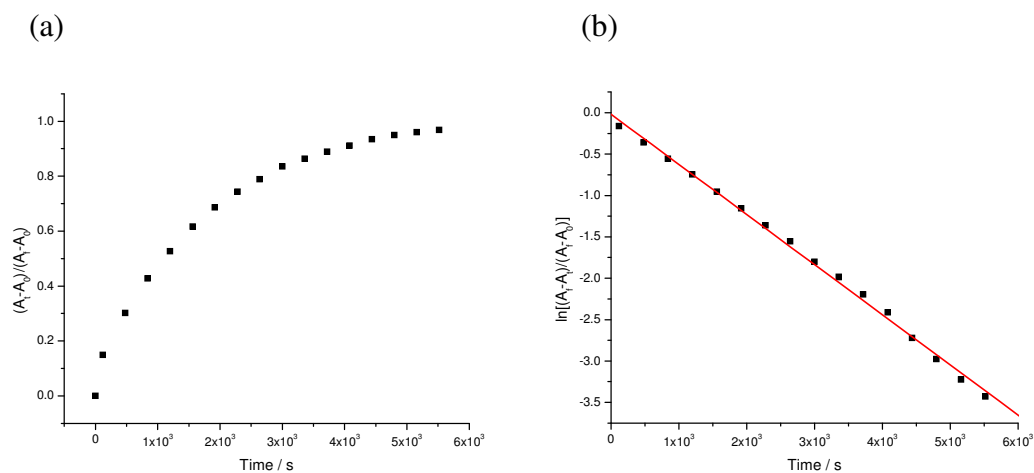


Table S1. k_{obs} for the reaction between complexes **1** and **3** in toluene solution with $[3] = 1.0 - 3.0 \text{ mmol L}^{-1}$ at 298 K.

$[3] \times 10^3 / \text{mol L}^{-1}$	$10^3 \times k_{obs} / \text{s}^{-1}$
1.0	0.80 ± 0.04
1.5	1.19 ± 0.06
2.0	1.69 ± 0.08
3.0	2.69 ± 0.13

Figure S4 Plot of k_{obs} vs. **[3]** at 298 K.

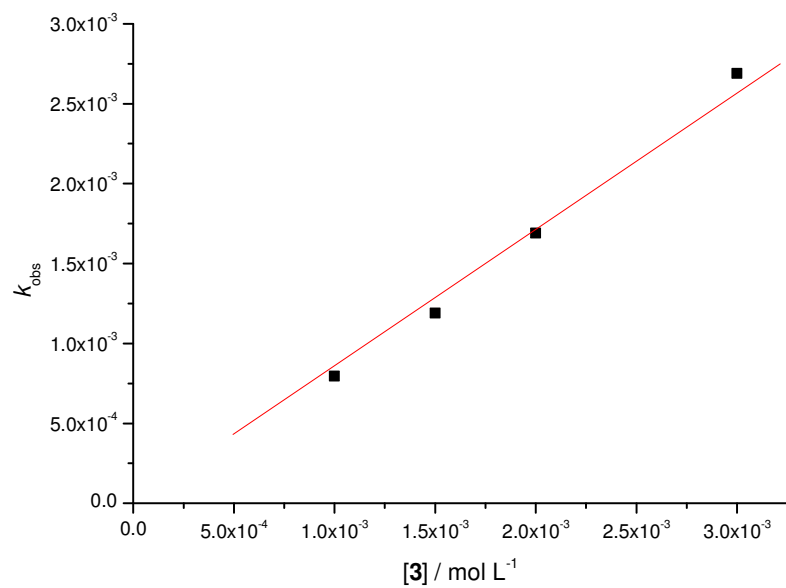


Table S2. k_2 for the reaction of **1** with **3** in toluene s at 291.5 – 314.0 K.

T / K	$10^4 \times k_2 / \text{L mol}^{-1} \text{s}^{-1}$
291.5	0.45 ± 0.02
298.0	0.72 ± 0.04
306.5	1.00 ± 0.05
314.0	1.48 ± 0.07

Figure S5. Eyring plot of $\ln(k_2/T)$ vs $1/T$ for reaction of **1** with **3** in toluene at 291.5 - 314 K. Activation parameters: $\Delta H^\ddagger = (8.8 \pm 1.6) \text{ kcal}\cdot\text{mol}^{-1}$ and $\Delta S^\ddagger = -(43.3 \pm 11.1) \text{ e.u.}$

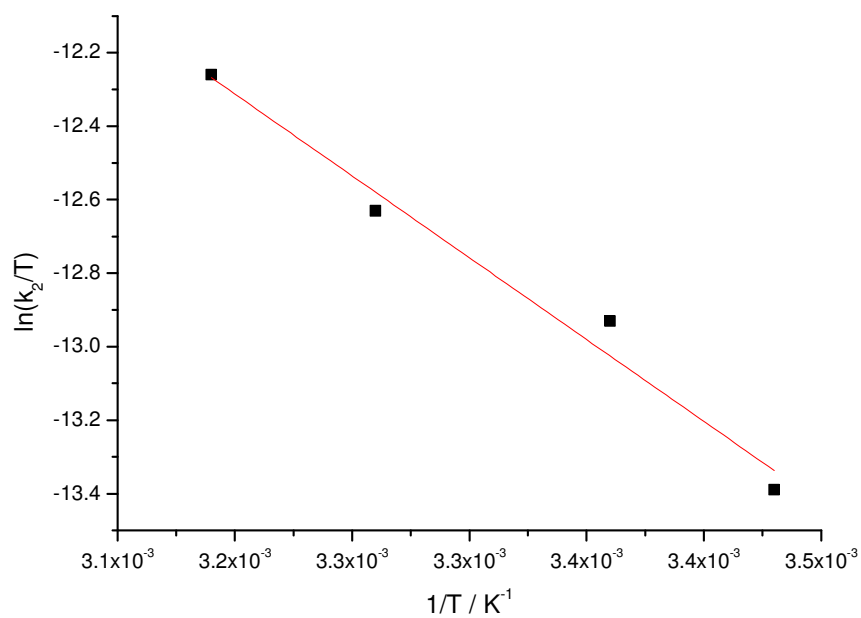


Table S3. Crystallographic data and experimental details for complexes **2** and **4**

	2	4
formula	C ₁₇ H ₃₈ Cl ₂ CoNO ₉ P ₃ Ru	C ₅₃ H ₈₆ Cl ₂ Co ₂ NO ₁₉ P ₇ Ru ₂
Fw	724.29	1648.92
<i>a</i> , Å	18.865(3)	16.3311(11)
<i>b</i> , Å	10.8115(17)	23.7167(17)
<i>c</i> , Å	28.320(4)	18.3823(12)
α , °	90	90
β , °	91.932(2)	100.870(7)
γ , °	90	90
<i>V</i> , Å ³	5772.9(16)	6992.1(8)
<i>Z</i>	8	4
Crystal system	Monoclinic	Monoclinic
space group	I2/a	P2 ₁ /n
<i>d</i> _{calc} , g cm ⁻³	1.667	1.566
<i>T</i> , K	100(2)	173(2)
μ , mm ⁻¹	1.492	9.852
<i>F</i> (000)	2952	3376
no. of refln	13601	45215
no. of indep. refln.	4860	12530
<i>R</i> _{int}	0.05	0.1419
<i>R</i> 1, <i>wR</i> 2 (<i>I</i> >2.0 σ (<i>I</i>))	0.0673, 0.170	0.0529, 0.0773
<i>R</i> 1, <i>wR</i> 2 (all data)	0.0856, 0.180	0.1377, 0.0968
Goodness of fit ^a	1.039	1.013

^a GoF = $[(\sum w|F_o| - |F_c|)^2 / (N_{\text{obs}} - N_{\text{param}})]^{1/2}$.

Table S4. Selected bond distances (Å) and angles (deg) for complex **2**.

Ru(1)-N(1)	2.061(6)	Ru(1)-Cl(1)	2.3209(18)
Ru(1)-Cl(2)	2.3351(19)	Ru(1)-O(7)	2.059(5)
Ru(1)-O(8)	2.073(5)	Ru(1)-O(9)	2.122(4)
Co(1)-P(1)	2.132(3)	Co(1)-P(2)	2.154(2)
Co(1)-P(3)	2.159(2)	Co(1)-C(1)	2.110(8)
Co(1)-C(2)	2.064(9)	Co(1)-C(3)	2.082(8)
Co(1)-C(4)	2.063(9)	Co(1)-C(5)	2.068(8)
O(7)-Ru(1)-N(1)	88.2(2)	O(7)-Ru(1)-O(8)	86.17(19)
O(7)-Ru(1)-O(9)	91.4(2)	O(7)-Ru(1)-Cl(1)	88.71(15)
O(7)-Ru(1)-Cl(2)	176.15(15)	O(8)-Ru(1)-O(9)	89.93(18)
O(8)-Ru(1)-Cl(1)	174.82(14)	O(8)-Ru(1)-Cl(2)	91.20(14)
O(9)-Ru(1)-Cl(1)	91.02(13)	O(9)-Ru(1)-Cl(2)	91.43(13)
N(1)-Ru(1)-O(8)	88.0(2)	N(1)-Ru(1)-O(9)	177.9(2)
N(1)-Ru(1)-Cl(1)	91.06(17)	N(1)-Ru(1)-Cl(2)	88.88(18)
Cl(1)-Ru(1)-Cl(2)	93.87(7)		

Table S5. Selected bond distances (Å) and angles (deg) for complex **4**.

Ru(1)-N(1)	1.818(6)	Ru(1)-Cl(1)	2.3625(19)
Ru(1)-Cl(2)	2.341(2)	Ru(1)-O(17)	2.119(5)
Ru(1)-O(18)	2.083(5)	Ru(1)-O(19)	2.143(5)
Ru(2)-N(1)	1.952(6)	Ru(2)-P(7)	2.327(2)
Ru(2)-C(81)	1.833(8)	Ru(2)-O(27)	2.152(5)
Ru(2)-O(28)	2.154(4)	Ru(2)-O(29)	2.165(5)
O(1)-C(81)	1.131(8)		
Ru(1)-N(1)-Ru(2)	153.6(3)	O(1)-C(81)-Ru(2)	176.5(8)
O(17)-Ru(1)-O(18)	86.47(18)	O(17)-Ru(1)-O(19)	87.63(18)
O(17)-Ru(1)-Cl(1)	175.92(14)	O(17)-Ru(1)-Cl(2)	92.05(15)
O(17)-Ru(1)-N(1)	96.8(2)	O(18)-Ru(1)-O(19)	85.23(17)
O(18)-Ru(1)-Cl(1)	91.57(13)	O(18)-Ru(1)-Cl(2)	170.00(13)
O(18)-Ru(1)-N(1)	95.3(2)	O(19)-Ru(1)-Cl(1)	88.65(14)
O(19)-Ru(1)-Cl(2)	84.82(14)	O(19)-Ru(1)-N(1)	175.6(2)
N(1)-Ru(1)-Cl(1)	86.98(18)	N(1)-Ru(1)-Cl(2)	94.71(18)
Cl(1)-Ru(1)-Cl(2)	89.27(7)	O(27)-Ru(2)-O(28)	82.86(17)
O(27)-Ru(2)-O(29)	83.15(17)	O(27)-Ru(2)-C(81)	93.6(3)
O(27)-Ru(2)-P(7)	92.10(14)	O(27)-Ru(2)-N(1)	166.4(2)
O(28)-Ru(2)-O(29)	85.24(18)	O(28)-Ru(2)-C(81)	176.3(3)
O(28)-Ru(2)-P(7)	94.07(14)	O(28)-Ru(2)-N(1)	85.1(2)
O(29)-Ru(2)-C(81)	93.5(3)	O(29)-Ru(2)-P(7)	175.25(12)
O(29)-Ru(2)-N(1)	89.4(2)	C(81)-Ru(2)-P(7)	86.9(3)
N(1)-Ru(2)-P(7)	95.23(17)	C(81)-Ru(2)-N(1)	98.3(3)